CONF-831174--66

LBL-16937

Lawrence Berkeley Laboratory
UNIVERSITY OF CALIFORNIA

Materials & Molecular Research Division

LBL--16937

DE84 005546

Presented at the 1983 Annual Meeting of the Materials Research Society, Boston, MA, November 14-17, 1983

ELECTRON MICROSCOPY AT ATOMIC RESOLUTION

R. Gronsky

November 1983

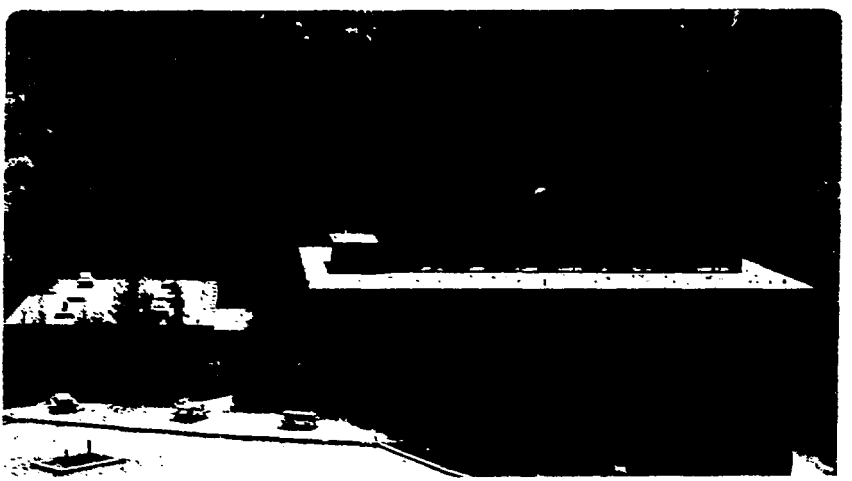

Prepared for the U.S. Department of Energy under Contract DE-AC03-76SF00098

ELECTRON MICROSCOPY AT ATOMIC RESOLUTION

R. Gronsky
National Center for Electron Microscopy
Materials and Molecular Research Division
Lawrence Berkeley Laboratory
University of California
Berkeley, California 94720

ABSTRACT

The direct imaging of atomic structure in solids has become increasingly easier to accomplish with modern transmission electron microscopes, many of which have an information retrieval limit near 0.2nm point resolution. Achieving better resolution, particularly with any useful range of specimen tilting, requires a major design effort. This presentation describes the new Atomic Resolution Microscope (ARM), recently put into operation at the Lawrence Berkeley Laboratory. Capable of 0.18nm or better "interpretable" resolution over a voltage range of 400 kV to 1000 kV with $\pm$ 40° biaxial specimen tilting, the ARM features a number of new electron-optical and microprocessor-control designs. These will be highlighted, and its atomic resolution performance demonstrated for a selection of inorganic crystals.

INTRODUCTION

In its most common mode of operation, the transmission electron microscope (TEM) produces images of thin specimens by an amplitude-contrast mechanism. Such images are formed by the utilization of a small objective aperture to admit only one scattered "beam" from the diffraction spectrum of the object through the microscope optics (Fig. 1(a) and (b)). Contrast under these conditions results from the spatial variation of the intensity distribution

contained within the chosen beam, and image resolution is determined by the extent to which the sampled scattering event is localized within the specimen.

Alternatively, thin specimen can be imaged in the TEM by a phase-contrast mechanism. This requires admitting more than one beam from the diffraction spectrum of the object through the microscope optics (Fig. 1(c)), and with proper setting of the objective lens current, the phase variations between the chosen beams are made to produce image contrast. Furthermore since these phase shifts are localized at the individual scattering species, image resolution is determined by the extent to which the complete diffraction spectrum is included in the imaging aperture, if all beams are included, atoms are resolved.

Although there have been no limitations on resolution imposed by instrumentation for quite some time in amplitude-contrast imaging, only the most modern TEM's have been successfully used for phase-contrast imaging of fine scale structure. Fortunately the sources of experimental difficulties which continue to prevent atomic resolution by this technique are also quite well known.

One set of problems has to do with beam-specimen interactions. In the phase-contrast imaging method, the specimen is frequently considered an integral part of the imaging optics since its only effect on the incident beam should be an alteration in phase[1]. This mandates that the object be very "thin", with the most severe constraints placed on preparing specimens of high atomic number. Other limitations include specimen orientation, irradiation damage,

both ionization and knock-on, and contamination under the illuminating beam from both the microscope vacuum environment and specimen-borne adsorbates.

Another set of problems stems from electron optics. Much like the specimen, the objective lens in the TEM affects the electron beam through an overall phase distortion. This phase change (X) in the diffraction spectrum is a function of scattering angle or position ($\underset{\sim}{u}$) in reciprocal space and can be written[2]

$$X(\underset{\sim}{u}) \approx \frac{2\pi}{\lambda}\left[C_s \frac{\lambda^4 u^4}{4} + \Delta z \frac{\lambda^2 u^2}{2}\right]$$

where λ is the electron wavelength, C_s the spherical aberration coefficient of the objective lens and Δz the defocus of the objective lens. Improving the contrast transfer characteristics of the objective lens therefore basically amounts to reducing λ and C_s while controlling Δz to match phases for the largest number of "beams" in the scattering distribution[3]. Attention must also be given to source coherence[4] and chromatic aberration[5] since these, too, serve to truncate the number of beams which can be effectively used during phase-contrast imaging.

ACHIEVING ATOMIC RESOLUTION

These combined effects impose limitations on the interpretation of phase-contrast images which are presently more severe than those imposed on their formation. Specifically, the point-to-point resolution of a microscope for directly interpretable images is established by the Scherzer defocus condition[6] whereby the phases of the electron waves scattered by the specimen are uniformly

controlled over the entire range of scattering vectors from $|\underset{\sim}{u}|=0$ to

$$|\underset{\sim}{u}| = [0.66\ C_s^{1/4}\ \lambda^{3/4}]^{-1}.$$

Another resolution limit is set however by the ultimate cut-off of spectra resulting from instrumental instabilities. This "information retrieval limit"[7] is characterized by fine detail in the image beyond the Scherzer limit where the phases of the electron waves scattered by the specimen are not uniformly controlled. For this reason the image is no longer "directly" interpretable; it must be viewed with accurate knowledge of the complete contrast transfer characteristics of the objective lens.

An approach to achieving atomic resolution in electron microscopy is therefore one of recognizing the present limitations of phase-contrast imaging and carefully interpreting or enhancing high resolution images in conjunction with computer simulations that account for instrumental shortcomings[8]. Alternatively, another approach is one of improving existing instrumentation. This was the course adopted by the recently completed Atomic Resolution Microscope (ARM) project[9,10] which is highlighted in the remainder of this review.

INSTRUMENTATION

The ARM (Fig. 2) is a high voltage electron microscope which has been designed for a point-to-point resolution consistently at or better than 0.18 nm over its entire 400 kV to 1000 kV accelerating potential range. Consequently the microscope can be tuned to a voltage which is below the threshold for knock-on damage in any specimen

of interest and used to directly image its contiguous atom structure. Voltage is generated by a Cockroft-Walton system using pressurized Freon insulation, with AC and DC columns concentrically disposed about the evacuated accelerating tube, all housed within a single tank. Both ripple and stability are maintained within 1 x 10^{-6} per minute using highly sensitive feedback compensation circuity. The instrument also has a unique vacuum system to control contamination, and employs two sputter ion pumps of capacity 1000 ℓ/sec each, backed by titanium sublimation pumps and turbomolecular pumps to maintain a pressure in the low 10^{-8} torr range throughout the electron-optical column and the accelerator tube.

To remove mechanical instabilities the microscope has been attached to a 100 ton inertial block and mounted on ten pneumatic isolators (Fig. 3) capable of dynamic leveling to within ± 0.001 inch from a preset value. The natural vibrational frequency of this system is 0.64 Hz in the horizontal plane and 1.15 Hz in the vertical.

Special attention has also been given to beam brightness in the ARM. At 1000 kV and 25 μA current, the LaB_6 cathodes in this microscope yield 10^8 amps/cm^2-str., enabling 2 sec. photographic exposure times at ∿300,000 x magnification. This level of brightness is furthermore preserved through the viewing glass (made under special subcontract by Nikon Optics) due to its tailored transmission coefficient which is matched to the wavelength of the photons emitted from the screen phosphor.

The key to the variable-voltage, atomic resolution performance of the ARM is its top entry objective stage, which, in addition to ± 40° biaxial tilting, incorporates a height (z) control to alter

specimen position along the optic axis over a 2 mm range within the objective lens. Using the z - control to focus the specimen, the microscope can be operated at the appropriate objective lens current which maintains a constant $C_s \lambda$ product for any accelerating voltage. This principle is in fact put into operation automatically on the ARM; the instantaneous orientation of the specimen is furthermore displayed via a graphics software package on the monitor screen (Fig. 4).

PERFORMANCE

The versatility of the high resolution, high angle goniometer of the ARM is demonstrated in Fig. 5. Moreover the z-control stage enables the specimen to be lowered within the lens pole piece to such an extent that the pre-field of the objective can be used as a probe-former. In this way, convergent beam electron diffraction (CBED) patterns can also be recorded from the same specimen areas imaged at high resolution (Fig. 6), providing greater precision in diffraction studies through the analysis of higher order Laue zone (HOLZ) lines[12].

Another effect of the height adjustable stage is its influence upon the optical properties of the objective lens. In general, the lens spherical aberration coefficient descreases with increasing lens excitation, although the exact functional variation is not a simple one[13]. At higher excitation, the lens focal length shortens, making it necessary to drop the specimen deeper into the focusing field. The most serious complication of this process is that the lens is physically constricted nearer the pole piece gap, and this

in turn reduces the maximum tilting range of the specimen goniometer. In the ARM, the specimen in its lowest z position is "restricted" to an otherwise generous ± 25° tilting range.

However the primary purpose of the height control is to optimize lens performance. An example of its proper use is shown in Fig. 7, the computed phase contrast transfer function for the ARM at 1000 kV operation with the specimen now located at an optimum 1.9 mm above its deepest immersion position. This calculation reveals that with proper care the ARM is theoretically capable of 0.13 nm point-to-point resolution.

Experimentally, the contrast transfer function of the ARM has been measured by the optical diffractogram method[14]. The 1 MeV results are shown in Fig. 8, where the point-to-point resolution is demonstrated to be 0.16 nm.

APPLICATIONS

The ARM accepts common 3 mm diameter specimens which have been thinned to electron transparency by standard techniques and screened for suitability in another TEM. Three cartridges can be simultaneously loaded into the specimen airlock and individually withdrawn by a turret mechanism for rapid insertion into the goniometer stage. Once in position, focusing and astigmatism correction are carried out while viewing the image directly on the screen phosphor. Through-focus series are facilitated by infinite-turn, continuously variable potentiometer control of the objective lens current, with a minimum focus increment of 0.3 nm. In addition, the stigmator coils are fed by six independent CPU channels, permitting different reference

settings to be stored in memory for rapid recall. Operation is further simplified by digital readout of all relevant lens and deflector coil excitation values at the console. Specific data concerning film number, operator code, magnification or camera length, and a 14 character text assigned by a user terminal are also recorded in the margin of each negative, of which there are 50 per camera load.

Two typical applications, one to an aluminum alloy, one to an ionic crystal, are presented in the last two figures.

SUMMARY

Current developments in atomic resolution microscopy are progressing rapidly on two fronts. One is the production of high precision microscopes in the medium ranges of accelerating potential (350 kV to 400 kV) which have the benefit of improved resolution and the advantage of a more compact size, increasing accessibility. The other is the extended use of image enhancement through real time video acquisition, digitization and computer processing for better signal-to-noise statistics. The latter approach obviously has higher potential for universal acceptance since it is not microscope-limited.

It should also be noted that there is essentially parallel activity in the further development of the scanning transmission electron microscope (STEM), which was intentionally omitted from this brief review. Although scanning beam systems continue to lag fixed beam systems in imaging quality, they offer outstanding advantages for complementary analyses, most notably in spatially-resolved spectroscopy.

Finally, it is the intention of the ARM project to continue

to urge the field of electron microscopy toward higher resolution while providing the field of materials science with a superior characterization tool[15]. Electron microscopy at atomic resolution is now both possible and extremely promising for materials research.

ACKNOWLEDGEMENTS

The author wishes to thank Dr. W. Krakow and the Program Committee for their kind invitation to present this review.

The Atomic Resolution Microscope is a User Facility supported by the Director, Office of Energy Research, Office of Basic Energy Sciences, Materials Science Division of the U.S. Department of Energy under Contract No. DE-AC03-76SF00098.

REFERENCES

1. S. Horiuchi, Ultramicroscopy 10, 229 (1982).

2. J. W. Goodman, Introduction to Fourier Optics, McGraw-Hill, New York (1968).

3. J. M. Cowley and A. F. Moodie, Proc. Phys. Soc. 76, 378 (1960).

4. J. Frank, Optik. 38, 519 (1973).

5. P. L. Fejes, Acta Cryst A33, 109 (1977).

6. O. Scherzer, J. Appl. Phys. 20, 20 (1949).

7. J.C.H. Spence, Experimental High Resolution Electron Microscopy, Clarendon Press, Oxford (1981).

8. W. O. Saxton, Computer Techniques and Image Processing in Electron Microscopy, Academic Press, New York (1978).

9. R. Gronsky in 38th. Annual Proc. Electron Microscopy Soc. Amer., San Francisco, G.W. Bailey (ed.), p. 2 (1980).

10. R. Gronsky and G. Thomas in 41st Annual Proc. Electron Microscopy Amer., Phoenix, G.W. Bailey (ed.), p. 310 (1983).

11. H. Watanabe, T. Honda, K. Tsuno, H. Kitajima, S. Katoh, Y. Baba, H. Kobayashi, N. Yoshimura, T. Itoh, Y. Harada, S. Sakurai, Y. Noguchi and T. Etoh in Proc. Seventh Int. Conf. on High Voltage Electron Microscopy, Berkeley, R. M. Fisher, R. Gronsky and K. H. Westmacott (eds.), p. 5 (1983).

12. J. W. Steeds in Introduction to Analytical Electron Microscopy, J. J. Hren, J. I. Goldstein and D. C. Joy (eds.), Plenum, New York, p. 387 (1979).

13. K. Tsuno and T. Honda, Optik 64, 367 (1983).

14. F. Thon, Z. Naturforsch 20a, 154 (1965).

15. A User's Guide to the National Center for Electron Microscopy is available upon request from M. Moore, NCEM, Lawrence Berkeley Laboratory, Berkeley, California 94720.

FIGURE CAPTIONS

Fig. 1. Ray diagram showing conditions for (a) bright field amplitude-contrast, (b) dark-field amplitude and (c) phase-contrast imaging.

Fig. 2. Console level view of the ARM. Large ion pump mount is visible on the upper left of the column; diagonal tube attached to left of specimen chamber is mass spectrometer head. Specimen exchange rod is attached horizontally to the right, and the manual controls for the goniometer descend the front of the column. The terminal at the lower right addresses all memory locations, digital console display and text field on micrograph negatives. Console controls are efficiently interfaced to the CPU, which reduces their total number.

Fig. 3. Side view of one half of the ARM vibration isolation system. The ten pneumatic isolators are located just below the console floor level, each carrying an average load of 27,130 lbs.

Fig. 4. Microcomputer and monitor used for specimen manipulation by keystroke control. Specimen position is indicated by digital readout and graphics display. Lower lines on monitor represent lens pole piece as height (z) reference.

Fig. 5. Results of ARM tilting experiment showing access to full crystallographic unit triangle of a silicon specimen.

Fig. 6. Central disc of CBED pattern from [011] silicon specimen.

Fig. 7. Computer phase contrast transfer function for the ARM, assuming 1000 kV accelerating voltage, C_S = 2.3 mm, C_C = 3.4 mm, defocus = 52 nm (Scherzer condition), and a disc-shaped source with a divergence half angle of 0.5 mrad and 2 eV energy spread.

At this imaging condition, the phases of all scattered waves are uniformly controlled over the widest range of scattering angles. The theoretical resolution limit is determined by the first crossover of the zero axis, here shown to be 0.13 nm.

Fig. 8 Optical diffractograms from high resolution images of (a) gold particles showing discrete 0.23, 0.20 and 0.14 nm reflections (left) and (b) amorphous Si (right) at Scherzer defocus, 1000 kV. The diffractogram halo in (b) is continuous out to a resolution limit of 0.16 nm.

Fig. 9 (a) (top) Atomic resolution image of a four atom layer γ' platelet in an Al-Ag alloy. The long particle dimension is 15 nm.

(b) (bottom) Atomic resolution image of an impingement event between γ' platelet and large ordered γ plate in an Al-Ag alloy. The impingement region again shows four atom layer stacking (arrow), demonstrating the role of Shockley partial dislocations in the growth process. Here the ledge mechanism is observed to be operable at the single atomic plane level.

Fig. 10 Ionic positions, electron diffraction pattern and atomic resolution image of a very thin section of barium titanate in an [001] zone axis orientation. The specimen was prepared by crushing in an agate mortar and suspending the powdered crystallites on a holey carbon support film. It was necessary to use the goniometer to tilt one of the crystallites which extended beyond the carbon film edge for this image, recorded at 1000 kV and -50 nm defocus.

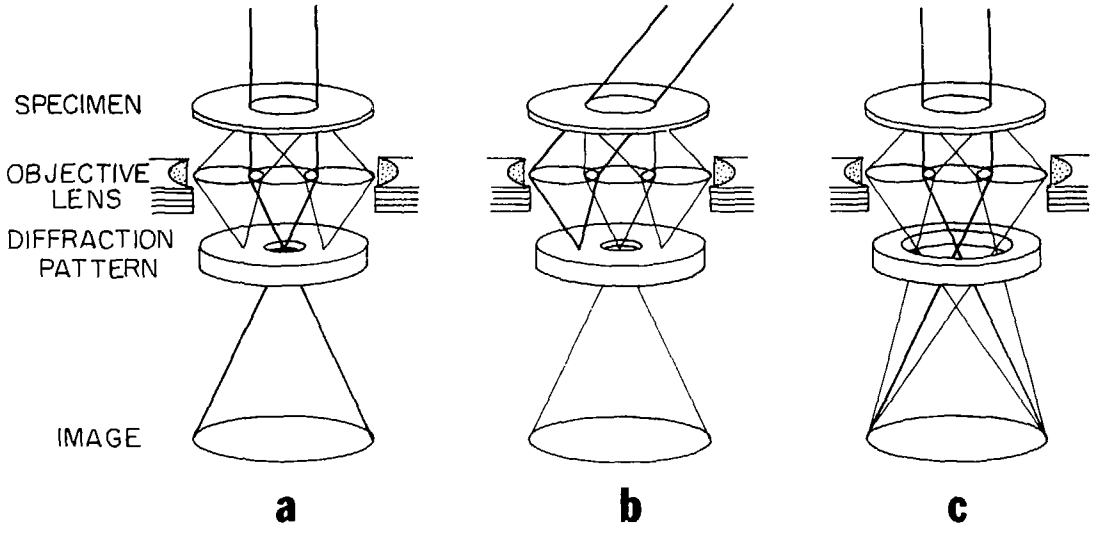

XBL 807-5497

Fig. 1

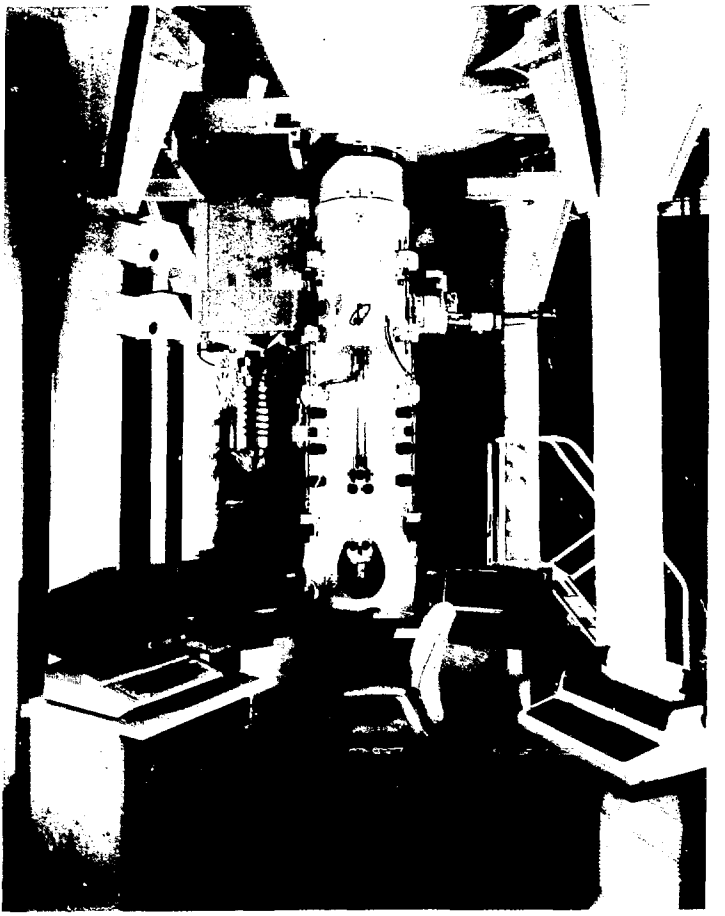

Fig. 2

CBB 833-2670

Fig. 3

Fig. 4

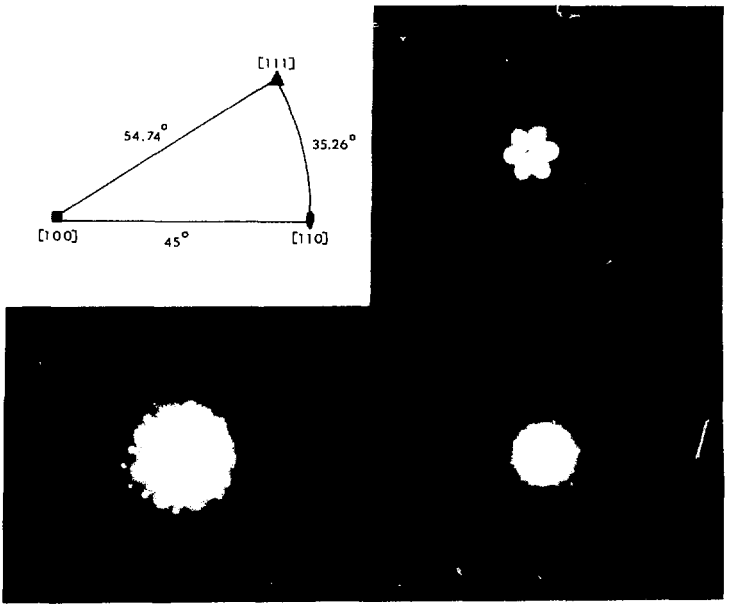

XBB 825-6031

Fig. 5

XBB [illegible]

Fig. 6

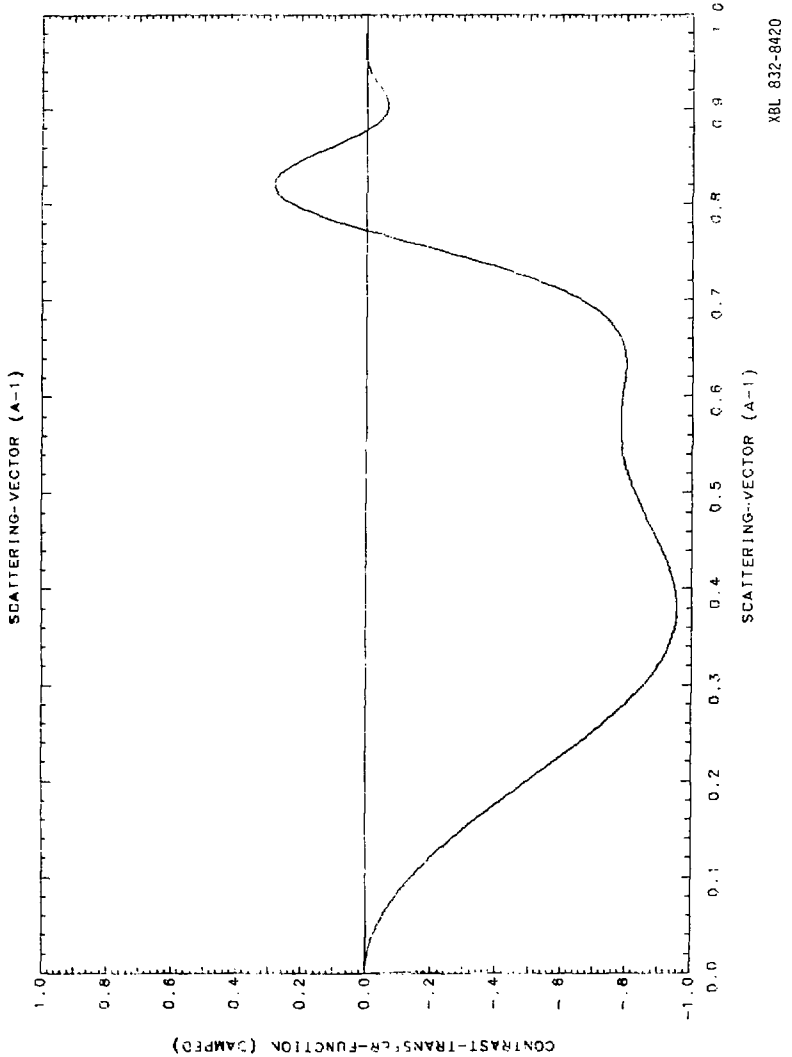
SCATTERING-VECTOR (A-1)
CONTRAST-TRANSFER-FUNCTION (DAMPED)
1.0
0.8
0.6
0.4
0.2
0.0
-.2
-.4
-.6
-.8
-1.0
0.0
0.1
0.2
0.3
0.4
0.5
0.6
0.7
0.8
0.9
1.0
SCATTERING-VECTOR (A-1)
XBL 832-8420

Fig. 7

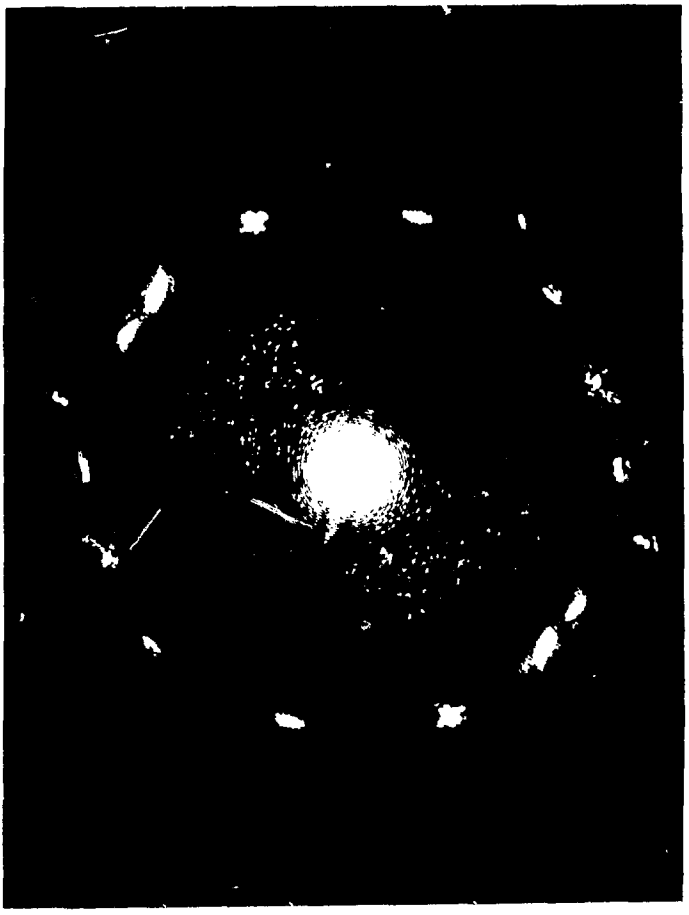

836-5045

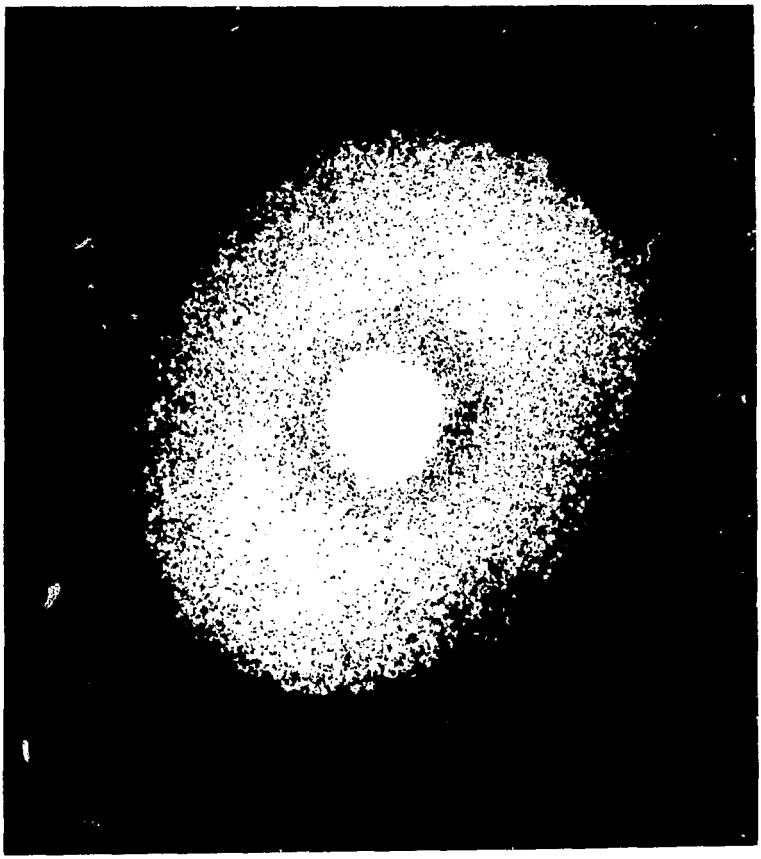

(b)
XBB 830-9044

Fig. 6

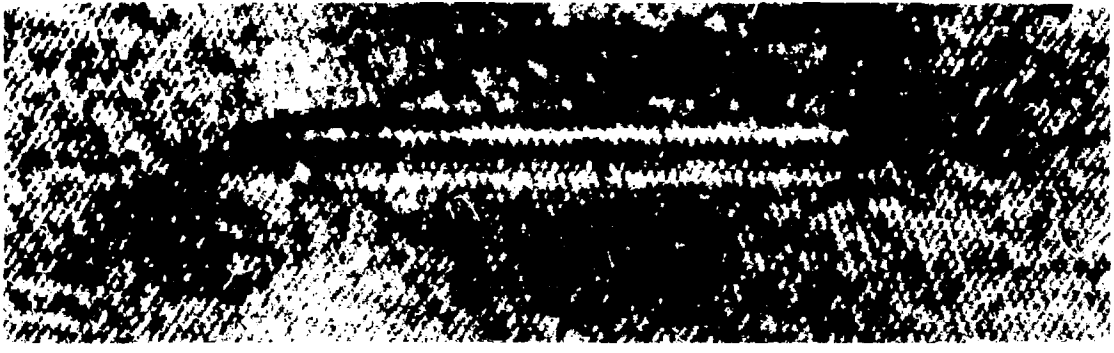

(a)

XBB 836-5046

Fig. 9

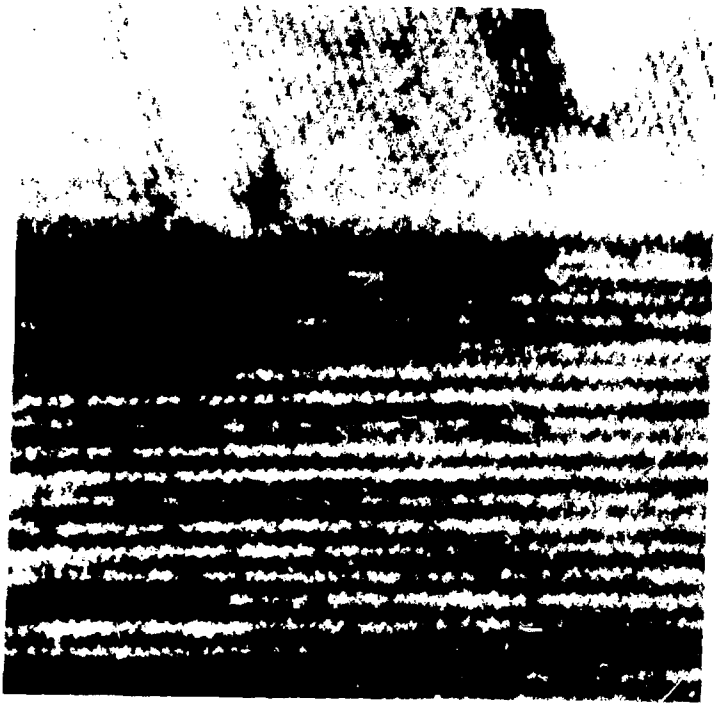

(b)
XBB 836-5041

Fig. 9

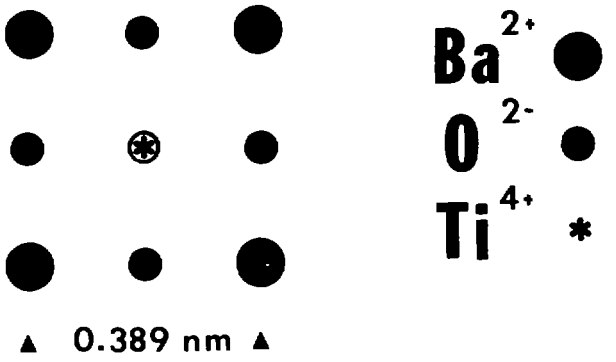

XBL 835-9630

Fig. 10(a)

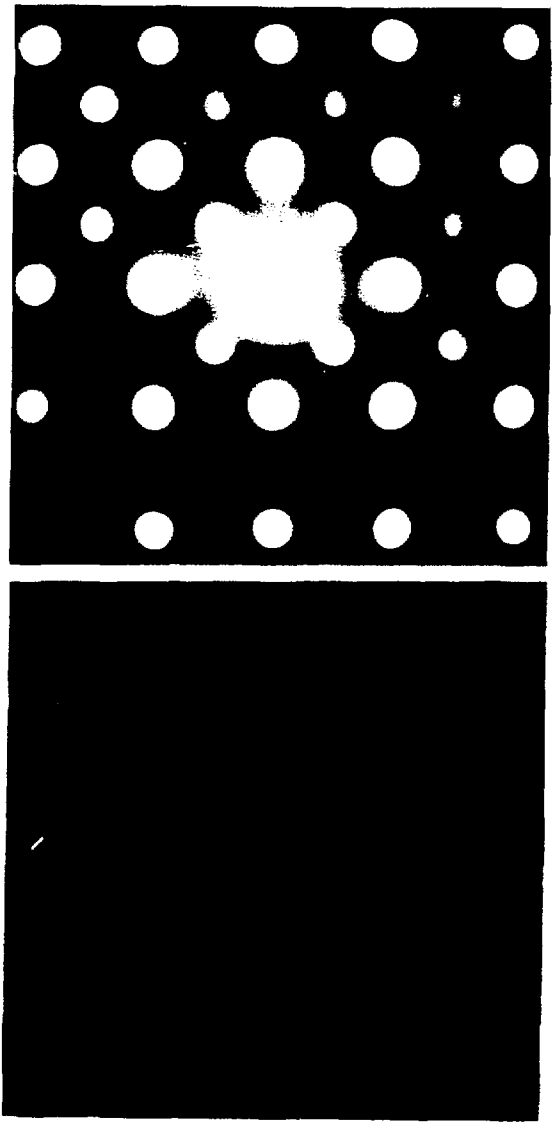

Fig. 10

(b,c)
XBB 836-5047